

Joint Uplink-Downlink Resource Allocation for OFDMA-URLLC MEC Systems

Walid R. Ghanem, Vahid Jamali, Qiuyu Zhang, and Robert Schober
Friedrich-Alexander-University Erlangen-Nuremberg, Germany

Abstract—In this paper, we study resource allocation algorithm design for multiuser orthogonal frequency division multiple access (OFDMA) ultra-reliable low latency communication (URLLC) in mobile edge computing (MEC) systems. To achieve the stringent end-to-end delay and reliability requirements of URLLC MEC systems, we propose joint uplink-downlink resource allocation and finite blocklength transmission. Furthermore, we propose a partial time overlap between the uplink and downlink frames to minimize the end-to-end delay, which introduces new time causality constraints. Then, the proposed resource allocation algorithm is formulated as an optimization problem for minimization of the total weighted transmit power of the network under constraints on the minimum quality-of-service regarding the number of computed URLLC user bits within the maximum allowable computing time, i.e., the end-to-end delay of a computation task. Due to the non-convexity of the optimization problem, finding the globally optimal solution entails a high computational complexity which is not tolerable for real-time applications. Therefore, a low-complexity algorithm based on successive convex approximation is proposed to find a high-quality sub-optimal solution. Our simulation results show that the proposed resource allocation algorithm design facilitates the application of URLLC in MEC systems, and yields significant power savings compared to a benchmark scheme.

I. INTRODUCTION

Future wireless communication networks have several system design objectives including high data rates, reduced latency, and massive device connectivity. One important objective is to enable ultra-reliable low latency communication (URLLC). URLLC will be widely adopted for mission-critical applications such as remote surgery, factory automation, autonomous driving, tactile Internet, and augmented reality to enable real-time machine-to-machine and human-to-machine interaction [1]. URLLC imposes strict quality-of-service (QoS) constraints including a very low latency (e.g., 1 ms) and a low packet error probability (e.g., 10^{-6}).

Recently, significant attention has been devoted to studying and developing resource allocation algorithms enabling URLLC. In particular, optimal power allocation in a multiuser time division multiple access (TDMA) URLLC system was considered in [2], [3]. Moreover, resource allocation for orthogonal frequency division multiple access (OFDMA)-URLLC systems was studied in [4]–[6]. However, the existing resource allocation schemes in [2], [3], [5], [6] focused only on communication while computation was not considered. Nevertheless, devices in mission-critical applications will also generate tasks that require computation within a given time. Therefore, resource allocation algorithm design for efficient computation in URLLC systems has to be investigated.

A promising solution to enable efficient and fast computation for URLLC devices is mobile edge computing (MEC). MEC enhances the battery lifetime and reduces the power consumption of users with delay-sensitive tasks. By offloading these tasks to nearby MEC servers, the power consumption and computation time at the local users can be considerably reduced at the expense of the power required for the data transmission for offloading. Thus, efficient resource allocation algorithm design is paramount for MEC for optimization of the available resources (e.g., power and bandwidth) while guaranteeing the maximum delay for the computation tasks. Existing resource allocation algorithms for MEC designs, such as [7], [8], were designed based on Shannon’s capacity formula. In particular, the authors in [7] studied energy-efficient resource allocation for MEC, while computation rate maximization was considered in [8]. However, if the resource allocation design for URLLC MEC systems is based on Shannon’s capacity formula, the reliability of the offloading and downloading processes cannot be guaranteed. To cope with this issue, recent works applied finite blocklength transmission (FBT) [9] for resource allocation algorithm design for URLLC MEC systems. In particular, the authors in [10] studied binary offloading in single-carrier TDMA systems. However, single-carrier systems suffer from poor spectrum utilization and require complex equalization at the receiver. In [11], the authors investigated the minimization of the normalized energy consumption for OFDMA. However, the algorithm proposed in [11] assumes that the channel gain is identical for different sub-carriers which may not be realistic for broadband wireless channels. Moreover, the resource allocation algorithms proposed in [11] are based on a simplified version of the general expression for the achievable rate for FBT [9]. Furthermore, the existing MEC designs, such as [7], [12], do not take into account the size of the computation result of the tasks and do not consider the communication resources consumed for downloading of the processed data by the users. Nevertheless, the size of the processed data can be large for applications such as augmented reality URLLC. To the best of the authors’ knowledge, joint uplink-downlink resource allocation for OFDMA-URLLC MEC systems has not been considered in the literature, yet.

Motivated by the above discussion, in this paper, we propose a novel power-efficient joint uplink-downlink resource allocation algorithm design for multiuser OFDMA-URLLC MEC systems. To reduce the end-to-end delay of the uplink and downlink transmission while efficiently exploiting the avail-

able spectrum, we propose a partial time overlap between the uplink and downlink frames which introduces new causality constraints. Then, the resource allocation algorithm design is formulated as an optimization problem for the minimization of the total weighted power consumed by the base station (BS) and the users subject to QoS constraints for the URLLC users. The QoS constraints include the minimum required number of bits computed within the maximum allowable time for computation, i.e., the maximum end-to-end delay of each user. The formulated optimization problem is a non-convex mixed-integer problem that is difficult to solve globally. Thus, we develop a low-complexity sub-optimal algorithm based on successive convex approximation (SCA) in order to find a locally optimal solution.

Notation: Lower-case letters x refer to scalar numbers, while bold lower-case letters \mathbf{x} represent vectors. $(\cdot)^T$ denotes the transpose operator. $\mathbb{R}^{N \times 1}$ represents the set of all $N \times 1$ vectors with real valued entries. The circularly symmetric complex Gaussian distribution with mean μ and variance σ^2 is denoted by $\mathcal{CN}(\mu, \sigma^2)$, \sim stands for “distributed as”, and $\mathcal{E}\{\cdot\}$ denotes statistical expectation. $\nabla_{\mathbf{x}}f(\mathbf{x})$ denotes the gradient vector of function $f(\mathbf{x})$ and its elements are the partial derivatives of $f(\mathbf{x})$.

II. SYSTEM AND CHANNEL MODELS

In this section, we present the considered system and channel models for OFDMA-URLLC MEC systems.

A. System Model

We consider a single-cell multiuser MEC system which comprises a BS and K URLLC users indexed by $k = \{1, \dots, K\}$, cf. Fig. 1. All transceivers have single antennas. The system employs frequency division duplex (FDD)¹. Thereby, the total bandwidth W is divided into two bands for uplink and downlink having bandwidths W^u and W^d , respectively. The bandwidths for uplink and downlink are further divided into M^u and M^d orthogonal sub-carriers indexed by $m^u = \{1, \dots, M^u\}$ and $m^d = \{1, \dots, M^d\}$, respectively. The bandwidth of each sub-carrier is BW_s . Thus, the symbol duration is $T_s = \frac{1}{BW_s}$. The uplink and downlink frames are divided into N^u time slots indexed by $n^u = \{1, \dots, N^u\}$ and N^d time slots indexed by $n^d = \{1, \dots, N^d\}$, respectively. Moreover, each time slot contains one OFDM symbol. The downlink transmission starts after τ time slots. Thus, uplink and downlink transmission overlap in $\bar{O} = N^u - \tau$ time slots. The value of τ is a design parameter. On the one hand, if τ is chosen too small, the users’ information bits to be computed may have not yet arrived at the BS and hence the downlink resource is wasted. On the other hand, if τ is chosen too large, the computed bits at the BS have to wait before being transmitted to the users, which increases the end-to-end delay, see Fig. 1. Each user has one computation task (B_k, D_k) that needs to be processed, where B_k is the task length in bits and D_k is the required time for computation in time slots.

¹In FDD systems, different frequency bands are assigned to uplink and downlink.

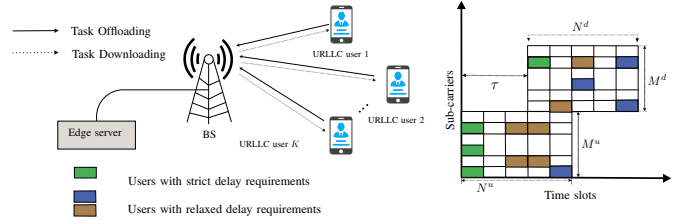


Figure 1: Multiuser MEC system with a single BS with an edge server and K URLLC users.

Moreover, we assume that all users offload their tasks to the MEC server. The maximum transmit power of the BS is P_{\max} , while the maximum transmit power of each user in the uplink is $P_{k,\max}$.

In order to facilitate the presentation, in the following, we use superscript $j \in \{u, d\}$ to denote uplink u and downlink d . *Remark 1.* The power and time consumed for channel estimation and resource allocation are constant and will not affect the validity of the proposed resource allocation algorithm. For simplicity of illustration, they are neglected in this paper. Furthermore, perfect channel state information (CSI) is assumed to be available at the BS for resource allocation design to obtain a performance upper bound for OFDMA-URLLC MEC systems.

B. Uplink and Downlink Channel Models

In the following, we introduce the uplink and downlink channel models for OFDMA-URLLC MEC systems. We assume that the channel gains of all users for all sub-carriers are constant during uplink and downlink transmission. In the uplink, the signal received at the BS from user k on sub-carrier m^u in time slot n^u is given as follows:

$$y_k^u[m^u, n^u] = h_k^u[m^u]x_k^u[m^u, n^u] + z_{BS}^u[m^u, n^u], \quad (1)$$

where $x_k^u[m^u, n^u]$ denotes the symbol transmitted by user k on sub-carrier m^u in time slot n^u to the BS. Moreover, $z_{BS}^u[m^u, n^u] \sim \mathcal{CN}(0, \sigma^2)$ denotes the noise at the BS², and $h_k^u[m^u]$ represents the complex channel coefficient between user k and the BS on sub-carrier m^u . Moreover, for future use, we define the signal-to-noise ratio (SNR) of user k 's signal at the input of the BS's receiver on sub-carrier m^u in time slot n^u as follows:

$$\gamma_k^u[m^u, n^u] = g_k^u[m^u]p_k^u[m^u, n^u], \quad (2)$$

where $p_k^u[m^u, n^u] = \mathcal{E}\{|x_k^u[m^u, n^u]|^2\}$ is the uplink transmitted power of user k on sub-carrier m^u in time slot n^u , and $g_k^u[m^u] = \frac{|h_k^u[m^u]|^2}{\sigma^2}$. A similar channel model is adopted for downlink transmission and the corresponding SNR at user k on sub-carrier m^d in time slot n^d is denoted by $\gamma_k^d[m^d, n^d]$.

C. Achievable Rate for FBT

Shannon's capacity theorem, on which most conventional resource allocation designs are based, applies to the asymptotic

²Without loss of generality, we assume that the noise processes at all receivers have identical variances.

case where the packet length approaches infinity and the decoding error probability goes to zero [13]. Thus, it cannot be used for resource allocation design for URLLC systems, as URLLC systems have to employ short packets to achieve low latency, which makes decoding errors unavoidable. For the performance evaluation of FBT, the so-called normal approximation for short packet transmission was developed in [14]. For parallel complex AWGN channels, the maximum number of bits Ψ conveyed in a packet comprising L symbols can be approximated as follows [14, Eq. (4.277)], [15, Fig. 1]:

$$\Psi = \sum_{l=1}^L \log_2(1 + \gamma[l]) - aQ^{-1}(\epsilon) \sqrt{\sum_{l=1}^L V[l]}, \quad (3)$$

where ϵ is the decoding packet error probability, and $Q^{-1}(\cdot)$ is the inverse of the Gaussian Q-function with $Q(x) = \frac{1}{\sqrt{2\pi}} \int_x^\infty \exp\left(-\frac{t^2}{2}\right) dt$. $V[l] = (1 - (1 + \gamma[l])^{-2})$ and $\gamma[l]$ are the channel dispersion [14] and the SNR of the l -th symbol, respectively, and $a = \log_2(e)$.

In this paper, we base the joint uplink-downlink resource allocation algorithm design for OFDMA-URLLC MEC systems on (3). By allocating several resource blocks from the available resources to a given user, the number of offloaded and downloaded bits of the user can be adjusted.

III. PROBLEM FORMULATION

In this section, we explain the offloading and downloading process and introduce the QoS requirements of the URLLC MEC users. Moreover, we formulate the proposed resource allocation optimization problem.

A. Offloading and Downloading

The edge computing process is performed as follows. First, each user offloads its data to the edge server in the uplink. Subsequently, the edge server processes this data and sends the results back in the downlink to the user. Thus, uplink and downlink should satisfy the following constraints:

$$C1 : \Psi_k^u(\mathbf{s}_k^u, \mathbf{p}_k^u) \geq B_k, \forall k, \quad C2 : \Psi_k^d(\mathbf{s}_k^d, \mathbf{p}_k^d) \geq \Gamma_k B_k, \forall k, \quad (4)$$

where

$$\Psi_k^j(\mathbf{s}_k^j, \mathbf{p}_k^j) = C_k^j(\mathbf{s}_k^j, \mathbf{p}_k^j) - V_k^j(\mathbf{s}_k^j, \mathbf{p}_k^j), \quad (5)$$

and

$$C_k^j(\mathbf{s}_k^j, \mathbf{p}_k^j) = \sum_{m^j=1}^{M^j} \sum_{n^j=1}^{N^j} s_k^j[m^j, n^j] \log_2(1 + \gamma_k^j[m^j, n^j]), \quad (6)$$

$$V_k^j(\mathbf{s}_k^j, \mathbf{p}_k^j) = aQ^{-1}(\epsilon_k^j) \sqrt{\sum_{m^j=1}^{M^j} \sum_{n^j=1}^{N^j} s_k^j[m^j, n^j] V_k^j[m^j, n^j]}. \quad (7)$$

Here, $s_k^j[m^j, n^j] = \{0, 1\}$, $\forall m^j, n^j$, are the sub-carrier assignment indicators. If sub-carrier m^j in time slot n^j is assigned to user k , we have $s_k^j[m^j, n^j] = 1$, otherwise $s_k^j[m^j, n^j] = 0$. Furthermore, we assume that each sub-carrier is allocated to at most one user to avoid multiple access interference.

$p_k^j[m^j, n^j]$ is the power allocated to user k on sub-carrier m^j in time slot n^j . \mathbf{s}_k^j and \mathbf{p}_k^j are the collections of optimization variables $s_k^j[m^j, n^j], \forall m^j, n^j$, and $p_k^j[m^j, n^j], \forall m^j, n^j, \forall j$, respectively, and $V_k^j[m^j, n^j] = (1 - (1 + \gamma_k^j[m^j, n^j])^{-2})$. Constraints C1 and C2 guarantee for user k the transmission of B_k bits in the uplink and $\Gamma_k B_k$ bits in the downlink, respectively. Moreover, $\Gamma_k, \forall k$, is the ratio of the sizes of the computation results and the offloaded task. The value of Γ_k depends on the application type, e.g., $\Gamma_k > 1$ is expected for augmented reality applications. [16].

B. Causality and Delay

In the following, we explain the causality and delay constraints.

1) *Causality*: According to Fig. 1, downlink transmission cannot start for a given user before all data of this user has been received at the BS via the uplink. Thus, we impose the following causality constraints³:

$$C3 : s_k^u[m^u, \tau + o] + s_k^d[m^d, n^d] \leq 1, \\ \forall o = \{1, \dots, \bar{O}\}, \forall k, \forall m^u, \forall n^d = \{1, \dots, o\}, \forall m^d. \quad (8)$$

This constraint ensures that the downlink transmission for a particular user cannot start before its data has arrived at the BS.

2) *Delay*: The delay of a computation task is limited by requiring the downlink transmission to be finished before $D_k - \tau$ time slots as follows:

$$C4 : s_k^d[m^d, n^d] = 0, \forall n^d \geq D_k - \tau. \quad (9)$$

The total latency of a computation task is determined by D_k and τ . Note that the values of D_k and τ are known for resource allocation.

C. Optimization Problem Formulation

In the following, we formulate the resource allocation design problem with the objective to minimize the total weighted network power consumption, while satisfying the latency requirements for the users' task computation. In particular, we optimize the power and sub-carrier assignments in uplink and downlink. To this end, the optimization problem is formulated as follows:

$$\min_{\mathbf{s}^u, \mathbf{p}^u, \mathbf{s}^d, \mathbf{p}^d} \sum_{k=1}^K w_k \sum_{m^u=1}^{M^u} \sum_{n^u=1}^{N^u} s_k^u[m^u, n^u] p_k^u[m^u, n^u] \quad (10) \\ + \sum_{k=1}^K \sum_{m^d=1}^{M^d} \sum_{n^d=1}^{N^d} s_k^d[m^d, n^d] p_k^d[m^d, n^d] \\ \text{s.t. } C1 - C4, \quad C5 : \sum_{k=1}^K s_k^u[m^u, n^u] \leq 1, \forall m^u, n^u, \\ C6 : s_k^u[m^u, n^u] \in \{0, 1\}, \forall k, m^u, n^u,$$

³In this paper, we neglect the computation time and power consumption at the edge server, and we only focus on uplink and downlink transmission. This model is valid when the edge server has sufficient processing and computation resources to carry out the small tasks of URLLC users.



Figure 2: Illustration of the key steps of the proposed low-complexity scheme.

$$\begin{aligned}
 \text{C7} : & \sum_{m^u=1}^{M^u} \sum_{n^u=1}^{N^u} s_k^u[m^u, n^u] p_k^u[m^u, n^u] \leq P_{k, \max}, \forall k, \\
 \text{C8} : & p_k^u[m^u, n^u] \geq 0, \forall k, m^u, n^u, \\
 \text{C9} : & \sum_{k=1}^K s_k^d[m^d, n^d] \leq 1, \forall m^d, n^d, \\
 \text{C10} : & s_k^d[m^d, n^d] \in \{0, 1\}, \forall k, m^d, n^d, \\
 \text{C11} : & \sum_{k=1}^K \sum_{m^d=1}^{M^d} \sum_{n^d=1}^{N^d} s_k^d[m^d, n^d] p_k^d[m^d, n^d] \leq P_{\max}, \\
 \text{C12} : & p_k^d[m^d, n^d] \geq 0, \forall k, m^d, n^d,
 \end{aligned}$$

where $s^j, \forall j$, and $\mathbf{p}^j, \forall j$, are the collections of optimization variables $s_k^j, \forall k, j$, and $\mathbf{p}_k^j, \forall k, j$, respectively. Moreover, $w_k \geq 1, \forall k$, are weights that allow the prioritization of the uplink power consumption compared to the downlink power consumption.

In (10), constraints C1 and C2 guarantee the transmission of a minimum number of bits from user k to the BS in the uplink and from the BS to user k in the downlink, respectively. Constraint C3 is the uplink-downlink causality constraint and constraint C4 ensures that user k is served within its delay requirements. Constraints C5 and C6 for the uplink and constraints C9 and C10 for the downlink are imposed to ensure that each sub-carrier in a given time slot is allocated to only one user. Constraints C7 and C11 are the total power constraints for user k and the BS, respectively. Constraints C8 and C12 are the non-negative transmit power constraints.

Optimization problem (10) is a mixed-integer non-convex problem. The non-convexity has the following reasons. First, the optimization variables in the objective function and the constraints are coupled, e.g., C1 and C7. Second, the achievable rate for FBT has a non-convex structure. Finally, the integer constraints C6, C10 are non-convex. In general, non-convex optimization problems cannot be solved optimally in polynomial time. Hence, in the next section, we focus on developing a sub-optimal solution, where the SCA method is employed for computational efficiency and real-time applicability.

IV. SOLUTION OF THE PROBLEM

In this section, we first transform the problem in (10) into a more tractable equivalent form. In particular, we first employ the Big-M formulation. Then, we use the difference of convex programming and SCA approaches in order to solve the optimization problem in (10) iteratively. The main steps of the proposed low-complexity algorithm are summarized in Fig. 2.

A. Problem Transformation

To deal with the non-convex product terms in optimization problem (10), the Big-M method is employed [17].

Step 1 (Big-M Formulation⁴): Let us introduce new optimization variables as

$$\bar{p}_k^j[m^j, n^j] = s_k^d[m^j, n^j] p_k^j[m^j, n^j], \forall k, m^j, n^j, \forall j. \quad (11)$$

Now, we decompose the product terms above using the Big-M formulation (McCormick envelopes) and impose the following additional constraints [18]:

$$\text{C13} : \bar{p}_k^u[m^u, n^u] \leq P_{k, \max} s_k^u[m^u, n^u], \forall k, m^u, n^u, \quad (12)$$

$$\text{C14} : \bar{p}_k^u[m^u, n^u] \leq p_k^u[m^u, n^u], \forall k, m^u, n^u, \quad (13)$$

$$\text{C15} : \bar{p}_k^u[m^u, n^u] \geq p_k^u[m^u, n^u] - (1 - s_k^u[m^u, n^u]) P_{k, \max}, \forall k, m^u, n^u, \quad (14)$$

$$\text{C16} : \bar{p}_k^u[m^u, n^u] \geq 0, \quad \forall k, m^u, n^u, \quad (15)$$

$$\text{C17} : \bar{p}_k^d[m^d, n^d] \leq P_{\max} s_k^d[m^d, n^d], \forall k, m^d, n^d, \quad (16)$$

$$\text{C18} : \bar{p}_k^d[m^d, n^d] \leq p_k^d[m^d, n^d], \quad \forall k, m^d, n^d, \quad (17)$$

$$\text{C19} : \bar{p}_k^d[m^d, n^d] \geq p_k^d[m^d, n^d] - (1 - s_k^d[m^d, n^d]) P_{\max}, \quad \forall k, m^d, n^d, \quad (18)$$

$$\text{C20} : \bar{p}_k^d[m^d, n^d] \geq 0, \quad \forall k, m^d, n^d. \quad (19)$$

The non-convex product terms $s_k^d[m^j, n^j] p_k^j[m^j, n^j], \forall k, m^j, n^j, \forall j$ in (11) are transformed into a set of convex linear inequalities. Note that constraints C13-C20 do not change the feasible set. Now, optimization problem (10) is transformed into the following equivalent form:

$$\begin{aligned}
 \min_{s^u, \mathbf{p}^u, s^d, \mathbf{p}^d, \bar{\mathbf{p}}^u, \bar{\mathbf{p}}^d} & \sum_{k=1}^K w_k \sum_{m^u=1}^{M^u} \sum_{n^u=1}^{N^u} \bar{p}_k^u[m^u, n^u] \\
 & + \sum_{k=1}^K \sum_{m^d=1}^{M^d} \sum_{n^d=1}^{N^d} \bar{p}_k^d[m^d, n^d] \\
 \text{s.t. C1} : & \bar{C}_k^u(\bar{\mathbf{p}}_k^u) - \bar{V}_k^u(\bar{\mathbf{p}}_k^u) \geq B_k, \forall k, \\
 \text{C2} : & \bar{C}_k^d(\bar{\mathbf{p}}_k^d) - \bar{V}_k^d(\bar{\mathbf{p}}_k^d) \geq \Gamma_k B_k, \forall k, \\
 \text{C3} - \text{C6, C7} : & \sum_{m^u=1}^{M^u} \sum_{n^u=1}^{N^u} \bar{p}_k^u[m^u, n^u] \leq P_{k, \max}, \forall k, \\
 \text{C8} - \text{C10, C11} : & \sum_{k=1}^K \sum_{m^d=1}^{M^d} \sum_{n^d=1}^{N^d} \bar{p}_k^d[m^d, n^d] \leq P_{\max}, \\
 & \text{C12, C13} - \text{C20.}
 \end{aligned} \quad (20)$$

where

$$\bar{C}_k^j(\bar{\mathbf{p}}_k^j) = \sum_{m^j=1}^{M^j} \sum_{n^j=1}^{N^j} \log_2(1 + \bar{\gamma}_k^j[m^j, n^j]), \quad (21)$$

$$\bar{V}_k^j(\bar{\mathbf{p}}_k^j) = \alpha Q^{-1}(\epsilon_k^j) \sqrt{\sum_{m^j=1}^{M^j} \sum_{n^j=1}^{N^j} \bar{V}_k^j[m^j, n^j]}, \quad (22)$$

⁴For more details on the big M-formulation, please refer to [18, Section 2.3].

$\bar{\gamma}_k^j[m^j, n^j] = g_k^j[m^j] \bar{p}_k^j[m^j, n^j]$, and $\bar{V}_k^j[m^j, n^j] = (1 - (1 + \bar{\gamma}_k^j[m^j, n^j])^{-2})$. Moreover, $\bar{\mathbf{p}}_k^j$ is the collection of optimization variables $\bar{p}_k^j[m^j, n^j], \forall m^j, n^j, \forall j$.

Optimization problem (20) is still non-convex. However, its structure is more tractable compared to problem (10). In the following, we find a low-complexity solution to problem (20) using the difference of convex programming and SCA methods.

B. Difference of Convex Programming

Step 2: The two remaining difficulties for solving problem (20) are the binary variables in constraints C6 and C10 and the structure of the achievable rate for FBT in C1 and C2. To tackle these issues, we employ a difference of convex (DC) programming approach [5], [17], [19], [20]. To this end, the integer constraints in (20) are rewritten in the following difference of convex function form:

$$\text{C6a} : 0 \leq s_k^u[m^u, n^u] \leq 1, \forall k, m^u, n^u, \quad (23)$$

$$\text{C6b} : E^u(\mathbf{s}^u) - H^u(\mathbf{s}^u) \leq 0, \quad (24)$$

$$\text{C10a} : 0 \leq s_k^d[m^d, n^d] \leq 1, \forall k, m^d, n^d, \quad (25)$$

$$\text{C10b} : E^d(\mathbf{s}^d) - H^d(\mathbf{s}^d) \leq 0, \quad (26)$$

where

$$E^j(\mathbf{s}^j) = \sum_{k=1}^K \sum_{m^j=1}^{M^j} \sum_{n^j=1}^{N^j} s_k^j[m^j, n^j], \forall j, \quad (27)$$

$$H^j(\mathbf{s}^j) = \sum_{k=1}^K \sum_{m^j=1}^{M^j} \sum_{n^j=1}^{N^j} (s_k^j[m^j, n^j])^2, \forall j. \quad (28)$$

Now, constraints C6, C10 have been rewritten in continuous form, cf. C6a, C10a. However, constraints C6b, C10b are non-convex, i.e., reverse convex constraints. In order to handle them, we introduce the following lemma.

Lemma 1. For sufficiently large constant values η_1 and η_2 the optimization problem in (20) is equivalent to the following problem:

$$\begin{aligned} & \underset{\mathbf{s}^u, \mathbf{p}^u, \mathbf{s}^d, \mathbf{p}^d, \bar{\mathbf{p}}^u, \bar{\mathbf{p}}^d}{\text{minimize}} \quad \Phi(\bar{\mathbf{p}}^u, \bar{\mathbf{p}}^d) + \eta_1(E^u - H^u) + \eta_2(E^d - H^d) \\ & \text{s.t.} \quad \text{C1} - \text{C5}, \text{C6a}, \text{C7} - \text{C9}, \text{C10a}, \text{C11} - \text{C20}, \end{aligned} \quad (29)$$

where $\Phi(\bar{\mathbf{p}}^u, \bar{\mathbf{p}}^d)$ is the objective function of problem (20).

Proof. Please refer to Appendix A. \blacksquare

The only remaining sources of non-convexity are the structure of the achievable rate for FBT and the non-convex objective function. In the following, we employ SCA to approximate problem (29) by a convex problem. Subsequently, we propose an iterative algorithm to find a low-complexity solution to problem (29).

C. Successive Convex Approximation

Step 3: In order to cope with the remaining non-convexity of (29), we employ the Taylor series approximation to approximate the non-convex parts of the objective function and

Algorithm 1 Successive Convex Approximation

- 1: Initialize: Random initial points $\mathbf{s}^{u(1)}, \mathbf{s}^{d(1)}, \bar{\mathbf{p}}^{u(1)}, \bar{\mathbf{p}}^{d(1)}$, set iteration index $i = 1$, maximum number of iterations I_{\max} , and initial penalty factors, $\eta_1 > 0$ and $\eta_2 > 0$.
 - 2: **Repeat**
 - 3: Solve convex problem (34) for given $\mathbf{s}^{u(i)}, \mathbf{s}^{d(i)}, \bar{\mathbf{p}}^{u(i)}, \bar{\mathbf{p}}^{d(i)}$, and store the intermediate solutions $\mathbf{s}^u, \mathbf{s}^d, \bar{\mathbf{p}}^u, \bar{\mathbf{p}}^d$
 - 4: Set $i = i + 1$ and update $\mathbf{s}^{u(i)} = \mathbf{s}^u, \mathbf{s}^{d(i)} = \mathbf{s}^d, \bar{\mathbf{p}}^{u(i)} = \bar{\mathbf{p}}^u, \bar{\mathbf{p}}^{d(i)} = \bar{\mathbf{p}}^d$.
 - 6: **Until** convergence or $i = I_{\max}$.
 - 7: **Output:** $\mathbf{s}^{u*} = \mathbf{s}^u, \mathbf{s}^{d*} = \mathbf{s}^d, \bar{\mathbf{p}}^{u*} = \bar{\mathbf{p}}^u, \bar{\mathbf{p}}^{d*} = \bar{\mathbf{p}}^d$.
-

constraints C1 and C2. Since $H^j(\mathbf{s}^j), \forall j$, and $-\bar{V}_k^j(\bar{\mathbf{p}}_k^j), \forall j$, are differentiable convex functions, then for any feasible points $\mathbf{s}^{j(i)}, \bar{\mathbf{p}}_k^{j(i)}, \forall j$, the following inequalities hold:

$$\begin{aligned} H^j(\mathbf{s}^j) & \geq \bar{H}^j(\mathbf{s}^j) = H^j(\mathbf{s}^{j(i)}) \\ & \quad + \nabla_{\mathbf{s}^j} H^j(\mathbf{s}^{j(i)})^T (\mathbf{s}^j - \mathbf{s}^{j(i)}), \forall j, \end{aligned} \quad (30)$$

and

$$\begin{aligned} \bar{V}_k^j(\bar{\mathbf{p}}_k^j) & \leq \tilde{V}_k^j(\bar{\mathbf{p}}_k^j, \bar{\mathbf{p}}_k^{j(i)}) = \bar{V}_k^j(\bar{\mathbf{p}}_k^{j(i)}) \\ & \quad + \nabla_{\bar{\mathbf{p}}_k^j} \bar{V}_k^j(\bar{\mathbf{p}}_k^{j(i)})^T (\bar{\mathbf{p}}_k^j - \bar{\mathbf{p}}_k^{j(i)}), \forall j. \end{aligned} \quad (31)$$

The right hand sides of (30) and (31) are affine functions representing the global underestimation of $H^j(\mathbf{s}^j), \forall j$, and $\bar{V}_k^j(\bar{\mathbf{p}}_k^j), \forall j$, respectively, where $\nabla_{\mathbf{s}^j} H^j(\mathbf{s}^{j(i)})^T (\mathbf{s}^j - \mathbf{s}^{j(i)})$ and $\nabla_{\bar{\mathbf{p}}_k^j} \bar{V}_k^j(\bar{\mathbf{p}}_k^{j(i)})$ are given on the top of the next page. By substituting the right hand sides of (30) and (31) into (29), we obtain the following optimization problem:

$$\begin{aligned} & \underset{\mathbf{s}^u, \mathbf{p}^u, \mathbf{s}^d, \mathbf{p}^d, \bar{\mathbf{p}}^u, \bar{\mathbf{p}}^d}{\text{minimize}} \quad \Phi(\bar{\mathbf{p}}^u, \bar{\mathbf{p}}^d) + \eta_1(E^u - \bar{H}^u) + \eta_2(E^d - \bar{H}^d) \\ & \text{s.t.} \quad \text{C1} : C_k^u(\bar{\mathbf{p}}_k^u) - \tilde{V}_k^u(\bar{\mathbf{p}}_k^u, \bar{\mathbf{p}}_k^{u(i)}) \geq B_k, \forall k, \\ & \quad \text{C2} : C_k^d(\bar{\mathbf{p}}_k^d) - \tilde{V}_k^d(\bar{\mathbf{p}}_k^d, \bar{\mathbf{p}}_k^{d(i)}) \geq \Gamma_k B_k, \forall k, \\ & \quad \text{C3} - \text{C5}, \text{C6a}, \text{C7} - \text{C9}, \text{C10a}, \text{C11} - \text{C20}. \end{aligned} \quad (34)$$

Optimization problem (34) is convex because the objective function is convex and the constraints span a convex set. Therefore, it can be efficiently solved by standard convex optimization solvers such as CVX [21]. Algorithm 1 summarizes the main steps to solve (29) in an iterative manner, where the solution of (34) in iteration (i) is used as the initial point for the next iteration ($i + 1$). The algorithm produces a sequence of improved feasible solutions until convergence to a local optimum point of problem (29) or equivalently problem (10) in polynomial time.

V. PERFORMANCE EVALUATION

In this section, we provide simulation results to evaluate the effectiveness of the proposed joint uplink-downlink resource allocation algorithm for OFDMA-URLLC MEC systems. We adopt the simulation parameters given in Table I, unless specified otherwise. In our simulations, a single cell is considered with inner and outer radii $r_1 = 50$ m and $r_2 = 100$ m,

$$\nabla_{\mathbf{s}^j} H^j(\mathbf{s}^{j(i)})^T (\mathbf{s}^j - \mathbf{s}^{j(i)}) = \sum_{k=1}^K \sum_{m^j=1}^{M^j} \sum_{n^j=1}^{N^j} 2s_k^{j(i)} [m^j, n^j] \left(s_k^j [m^j, n^j] - s_k^{j(i)} [m^j, n^j] \right), \forall j, \quad (32)$$

$$\nabla_{\bar{\mathbf{P}}_k^j} \bar{V}_k^j(\bar{\mathbf{P}}_k^j) = \frac{aQ^{-1}(\epsilon_k^j)}{\sqrt{\sum_{m^j=1}^{M^j} \sum_{n^j=1}^{N^j} \bar{V}_k^j(i) [m^j, n^j]}} \begin{pmatrix} \frac{g_k^j[1]}{(1+\bar{p}_k^{j(i)}[1,1]g_k^j[1])^3} \\ \vdots \\ \frac{g_k^j[M]}{(1+\bar{p}_k^{j(i)}[M,N]g_k^j[M])^3} \end{pmatrix}, \forall j. \quad (33)$$

Table I: Simulation Parameters.

Parameter	Value
Total number of sub-carriers in uplink and downlink $M = M^u = M^d$	$2M=64$
Number of time slots in uplink and downlink $N^u = N^d$	4
Bandwidth of each sub-carrier	30 kHz
Noise power density	-174 dBm/Hz
Maximum BS transmit power, P_{\max}	45 dBm
Maximum transmitted power of each user, $P_{k,\max}$	23 dBm
Value of $\Gamma_k, \forall k$	1

respectively. The BS is located at the center of the cell, and the users are randomly located between the inner and the outer radii. The user weights are set to $w_k = 1, \forall k$ for simplicity. The path loss is calculated as $35.3 + 37.6 \log_{10}(d_k)$ [22], where d_k is the distance from the BS to user k . The values of the penalty factors are set to $\eta_1 = 10K P_{k,\max}$ and $\eta_2 = 10P_{\max}$. The small scale fading gains between the BS and the users are modeled as independent and identically Rayleigh distributed. All simulation results are averaged over 100 realizations of the path loss and multipath fading.

A. Performance Bound and Benchmark Scheme

We compare the performance of the proposed resource allocation algorithm with the following benchmark schemes:

- **Shannon's capacity (SC):** To obtain an (unachievable) lower bound on the total network power consumption, Shannon's capacity formula is adopted in problem (10), i.e., $V_k^j(\mathbf{s}_k^j, \mathbf{P}_k^j), \forall j$, is set to zero in constraints C1 and C2, respectively, and all other constraints are retained. The resulting optimization problem is solved using a modified version of the proposed algorithm.
- **Fixed sub-carrier assignment (FSA):** In this scheme, we fix the sub-carrier assignment. In fact, we divide the total number of sub-carriers among the users such that their delay and causality constraints are met. Then, we optimize the power allocated to the sub-carriers for the given channel realization. The resulting optimization problem is solved using the SCA method.

B. Simulation Results

In Fig. 3, we investigate the average system power consumption versus the size of the task of the URLLC users and study the impact of different delay requirements. For delay scenario S_0 , none of the users has delay restrictions, i.e., $D_k = \tau + N^d = 7, \forall k$. In contrast, for delay scenario S_1 , two users have strict delay constraints while the remaining users do not, i.e., $D_1 = D_2 = 5$ and $D_3 = D_4 = 7$. As expected, increasing the required number of transmitted bits leads to higher transmit powers. This is due to the fact that if more bits are to be transmitted in a given frame, higher SNRs

are needed, and thus, the BS and the users have to increase the transmitted power. Furthermore, the proposed scheme leads to a substantially lower power consumption compared to the FSA scheme. This is due to the non-optimal sub-carrier allocation for the FSA scheme. Fig. 3 also reveals the impact of strict delay requirements. In particular, delay scenario S_1 leads to a higher power consumption compared to S_0 because the BS and the users are forced to allocate more power even if their channel conditions are poor to ensure their transmissions are completed with the desired delay. Furthermore, SC provides a lower bound for the required power consumption of OFDMA-URLLC MEC systems. However, SC cannot guarantee the required latency and reliability. This is due to the fact that, in this scheme, the performance loss incurred by FBT is not taken into account for resource allocation design, and thus the obtained resource allocation policies may not meet the QoS constraints.

In Fig. 4, we show the average system power consumption versus the packet error probability and study the impact of different delay requirements. As can be observed, for the proposed scheme and FSA, the average system power consumption is a monotonically decreasing function of the packet error probability. This is due to the fact that the complementary error function in the normal approximation is a monotonically decreasing function of ϵ , and as a result, the impact of the dispersion part in the normal approximation decreases as ϵ increases. Fig. 4 also reveals the impact of delay constraints. In particular, delay scenario $\bar{S}_1 = \{D_1 = D_2 = D_3 = 5, D_4 = D_5 = 7\}$ leads to a higher power consumption compared to $\bar{S}_0 = \{D_k = 7, \forall k\}$. This is due to the smaller feasible set of the optimization problem. Moreover, as can be seen, for SC, the power consumption is independent of the packet error probability. This is due to the fact that SC assumes that the decoding error probability is zero. Moreover, the gap between the proposed scheme and SC is the price to be paid for enforcing strict delay and reliability requirements to ensure URLLC.

VI. CONCLUSIONS

This paper studied the resource allocation algorithm design for OFDMA-URLLC MEC systems. To ensure the stringent end-to-end transmission delay and reliability requirements of URLLC, we proposed a joint uplink-downlink resource allocation scheme which takes into account FBT. Moreover, to minimize the end-to-end delay, we proposed a partial time overlap between the uplink and downlink frames which introduces new uplink-downlink causality constraints. The proposed resource allocation algorithm design was formulated as an optimization

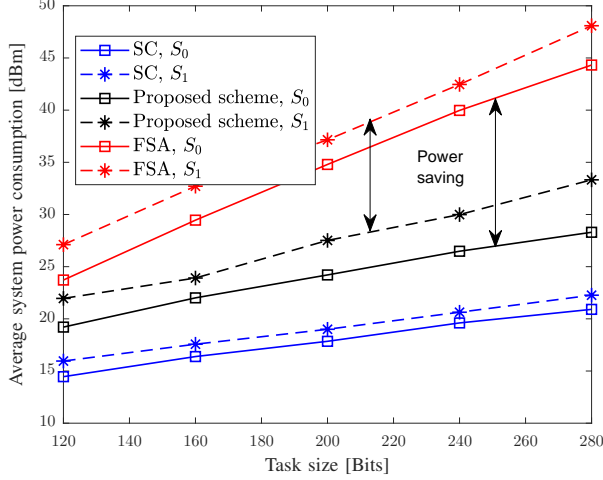


Figure 3: Average consumed power [dBm] vs. task size [bits], $K = 4$, $\tau = 3$, $\bar{O} = 1$, $\epsilon_k^j = 10^{-6}$, $\forall j, k$.

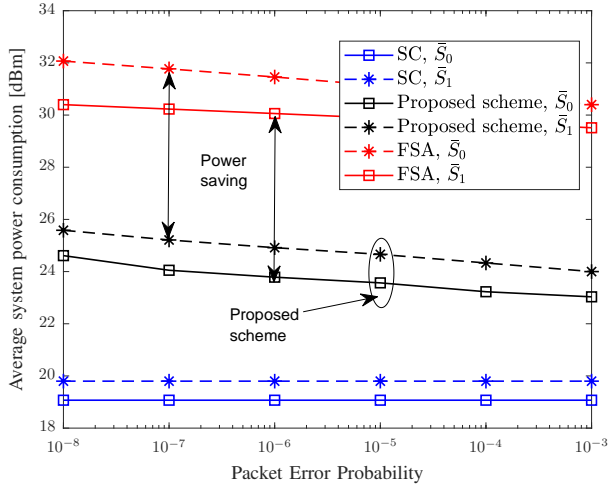


Figure 4: Average consumed power [dBm] vs. packet error probability, $K = 5$, $\tau = 3$, $\bar{O} = 1$, $B_k = 160$ bits, $\forall k$.

problem for minimization of the total weighted transmit power of the network under QoS constraints regarding the minimum required number of computed bits of the URLLC users within a maximum computing time, i.e., the end-to-end delay. Due to the non-convexity of the formulated problem, finding a global solution entails a prohibitive computational complexity. Thus, a low-complexity algorithm based on SCA was proposed to find a high-quality sub-optimal solution. Our simulation results showed that the proposed resource allocation algorithm design facilitates the application of URLLC in MEC systems, and achieves significant power savings compared to a benchmark scheme.

APPENDIX A

The proof follows similar steps as corresponding proofs in [5], [17], [19]. In the following, we show that problems (29) and (20) are equivalent. Let U^* denote the optimal objective

value of (29). We define the Lagrangian function, denoted by $\mathcal{L}(\bar{\mathbf{p}}^u, \bar{\mathbf{p}}^d, \mathbf{s}^u, \mathbf{s}^d, \eta_1, \eta_2)$, as [23]

$$\mathcal{L}(\bar{\mathbf{p}}^u, \bar{\mathbf{p}}^d, \mathbf{s}^u, \mathbf{s}^d, \eta_1, \eta_2) = \Phi(\bar{\mathbf{p}}^u, \bar{\mathbf{p}}^d) + \eta_1(E^u - H^u) + \eta_2(E^d - H^d), \quad (35)$$

where η_1 and η_2 are the Lagrange multipliers corresponding to constraints C6b and C10b, respectively. Note that $E^u(\mathbf{s}^u) - H^u(\mathbf{s}^u) \geq 0$ and $E^d(\mathbf{s}^d) - H^d(\mathbf{s}^d) \geq 0$ hold. Using Lagrange duality [5], [20], [23], we have the following relation⁵

$$U_d^* = \max_{\eta_1, \eta_2 \geq 0} \min_{\mathbf{p}^u, \mathbf{p}^d, \mathbf{s}^u, \mathbf{s}^d, \bar{\mathbf{p}}^u, \bar{\mathbf{p}}^d \in \Omega} \mathcal{L}(\bar{\mathbf{p}}^u, \bar{\mathbf{p}}^d, \mathbf{s}^u, \mathbf{s}^d, \eta_1, \eta_2) \quad (36)$$

$$\stackrel{(a)}{\leq} \min_{\mathbf{p}^u, \mathbf{p}^d, \mathbf{s}^u, \mathbf{s}^d, \bar{\mathbf{p}}^u, \bar{\mathbf{p}}^d \in \Omega} \max_{\eta_1, \eta_2 \geq 0} \mathcal{L}(\bar{\mathbf{p}}^u, \bar{\mathbf{p}}^d, \mathbf{s}^u, \mathbf{s}^d, \eta_1, \eta_2) = U^*, \quad (37)$$

where Ω is the feasible set specified by the constraints in (29). In the following, we first prove the strong duality, i.e., $U_d^* = U^*$. Let $(\mathbf{p}^{u*}, \mathbf{p}^{d*}, \mathbf{s}^{u*}, \mathbf{s}^{d*}, \bar{\mathbf{p}}^{u*}, \bar{\mathbf{p}}^{d*}, \eta_1^*, \eta_2^*)$ denotes the solution of (36). For this solution, the following two cases are possible. *Case 1*) If $E^u(\mathbf{s}^u) - H^u(\mathbf{s}^u) > 0$ and $E^d(\mathbf{s}^d) - H^d(\mathbf{s}^d) > 0$ hold, the optimal η_1^* and η_2^* are infinite, respectively. Hence, U_d^* is infinite too, which contradicts the fact that it is upper bounded by a finite-value U^* . *Case 2*) If $E^u(\mathbf{s}^u) - H^u(\mathbf{s}^u) = 0$ and $E^d(\mathbf{s}^d) - H^d(\mathbf{s}^d) = 0$ hold, then $(\mathbf{p}^{u*}, \mathbf{p}^{d*}, \mathbf{s}^{u*}, \mathbf{s}^{d*}, \bar{\mathbf{p}}^{u*}, \bar{\mathbf{p}}^{d*})$ belongs to the feasible set of the original problem (20) which implies $U_d^* = U^*$. Hence, strong duality holds, and we can focus on solving the dual problem (36) instead of the primal problem (37).

Next, we show that any $\eta_1 \geq \eta_{1,0}$ and $\eta_2 \geq \eta_{2,0}$ are optimal solutions for dual problem (36), i.e., η_1^* and η_2^* , where $\eta_{1,0}$ and $\eta_{2,0}$ are some sufficiently large numbers. To do so, we show that $\Theta(\eta_1, \eta_2) \triangleq \min_{\bar{\mathbf{p}}^u, \bar{\mathbf{p}}^d, \mathbf{p}^u, \mathbf{p}^d, \mathbf{s}^u, \mathbf{s}^d \in \Omega} \mathcal{L}(\bar{\mathbf{p}}^u, \bar{\mathbf{p}}^d, \mathbf{s}^u, \mathbf{s}^d, \eta_1, \eta_2)$ is a monotonically increasing function of η_1 and η_2 . Recall that $E^u(\mathbf{s}^u) - H^u(\mathbf{s}^u) \geq 0$ and $E^d(\mathbf{s}^d) - H^d(\mathbf{s}^d) \geq 0$ holds for any given $\mathbf{p}^u, \mathbf{p}^d, \mathbf{s}^u, \mathbf{s}^d, \bar{\mathbf{p}}^u, \bar{\mathbf{p}}^d \in \Omega$. Therefore, $\mathcal{L}(\bar{\mathbf{p}}^u, \bar{\mathbf{p}}^d, \mathbf{s}^u, \mathbf{s}^d, \eta_1(1), \eta_2(1)) \leq \mathcal{L}(\bar{\mathbf{p}}^u, \bar{\mathbf{p}}^d, \mathbf{s}^u, \mathbf{s}^d, \eta_1(2), \eta_2(2))$ holds for any given $\bar{\mathbf{p}}^u, \bar{\mathbf{p}}^d, \mathbf{p}^u, \mathbf{p}^d, \mathbf{s}^u, \mathbf{s}^d \in \Omega$, $0 \leq \eta_1(1) \leq \eta_1(2)$, and $0 \leq \eta_2(1) \leq \eta_2(2)$. This implies that $\Theta(\eta_1(1), \eta_2(1)) \leq \Theta(\eta_1(2), \eta_2(2))$ and that $\Theta(\eta_1, \eta_2)$ is monotonically increasing in η_1 and η_2 . Using this result, we can conclude that $\Theta(\eta_1, \eta_2) = U^*$, $\forall \eta_1 \geq \eta_{1,0}, \eta_2 \geq \eta_{2,0}$.

In summary, due to strong duality, we can use the dual problem (29) to find the solution of the primal problem (20) and any $\eta_1 \geq \eta_{1,0}$ and $\eta_2 \geq \eta_{2,0}$ are optimal dual variables. These results are concisely given in Lemma 1 which concludes the proof.

REFERENCES

- [1] P. Popovski, "Ultra-reliable communication in 5G wireless systems," in *Proc. IEEE Int. Conf. 5G Ubiqu. Connect.*, Nov 2014, pp. 146–151.

⁵Note that weak duality holds for convex and non-convex optimization problems [23].

- [2] Y. Hu, M. Ozmen, M. C. Gursoy, and A. Schmeink, "Optimal power allocation for QoS-constrained downlink multi-user networks in the finite blocklength regime," *IEEE Trans. Wireless Commun.*, vol. 17, no. 9, pp. 5827–5840, Sept 2018.
- [3] S. Xu, T. H. Chang, S. C. Lin, C. Shen, and G. Zhu, "Energy-efficient packet scheduling with finite blocklength codes: convexity analysis and efficient algorithms," *IEEE Trans. Wireless Commun.*, vol. 15, no. 8, pp. 5527–5540, Aug 2016.
- [4] C. She, C. Yang, and T. Q. S. Quek, "Joint uplink and downlink resource configuration for ultra-reliable and low-latency communications," *IEEE Trans. Commun.*, vol. 66, no. 5, pp. 2266–2280, May 2018.
- [5] W. Ghanem, V. Jamali, Y. Sun, and R. Schober, "Resource allocation for multi-user downlink URLLC-OFDMA systems," in *Proc. IEEE Int. Commun. Conf.*, Shanghai, P.R. China, May 2019.
- [6] W. R. Ghanem, V. Jamali, Y. Sun, and R. Schober, "Resource allocation for multi-user downlink MISO OFDMA-URLLC systems," 2019, Submitted to IEEE Trans. Commun., <https://arxiv.org/abs/1910.06127>.
- [7] Z. Yang, C. Pan, J. Hou, and M. Shikh-Bahaei, "Efficient resource allocation for mobile-edge computing networks with NOMA: completion time and energy minimization," *IEEE Trans. Commun.*, vol. 67, no. 11, pp. 7771–7784, Nov 2019.
- [8] F. Zhou and R. Q. Hu, "Computation efficiency maximization in wireless-powered mobile edge computing networks," *IEEE Trans. Wirel. Commun.*, pp. 1–1, Early access, 2020.
- [9] Y. Polyanskiy, H. V. Poor, and S. Verdú, "Channel coding rate in the finite blocklength regime," *IEEE Trans. Inf. Theory*, vol. 56, no. 5, pp. 2307–2359, May 2010.
- [10] M. Salmani and T. N. Davidson, "On multi-user binary computation offloading in the finite-block-length regime," in *Proc. 53rd Asilomar Conf. Signals, Systems, and Computers*, 2019, pp. 378–382.
- [11] R. Dong, C. She, W. Hardjawana, Y. Li, and B. Vucetic, "Deep learning for hybrid 5G services in mobile edge computing systems: Learn from a digital twin," *IEEE Trans. Wirel. Commun.*, vol. 18, no. 10, pp. 4692–4707, Oct 2019.
- [12] Y. Zhou, C. Pan, P. L. Yeoh, K. Wang, M. ElKashlan, B. Vucetic, and Y. Li, "Secure communications for UAV-enabled mobile edge computing systems," *IEEE Trans. Commun.*, vol. 68, no. 1, pp. 376–388, Jan 2020.
- [13] C. E. Shannon, "A mathematical theory of communication," *Bell Syst. Tech. J.*, vol. 56, no. 5, pp. 2307–2359, May 2010.
- [14] Y. Polyanskiy, "Channel coding: Non-asymptotic fundamental limits," Ph.D. dissertation, Princeton University.
- [15] T. Erceghe, "Coding in the finite-blocklength regime: Bounds based on Laplace integrals and their asymptotic approximations," *IEEE Trans. Inf. Theory*, vol. 62, no. 12, pp. 6854–6883, Dec 2016.
- [16] W. Wen, Y. Fu, T. Q. S. Quek, F. Zheng, and S. Jin, "Joint uplink/downlink sub-channel, bit and time allocation for multi-access edge computing," *IEEE Commun. Lett.*, vol. 23, no. 10, pp. 1811–1815, Oct 2019.
- [17] Y. Sun, D. W. K. Ng, Z. Ding, and R. Schober, "Optimal joint power and subcarrier allocation for full-duplex multicarrier non-orthogonal multiple access systems," *IEEE Trans. Commun.*, vol. 65, no. 3, pp. 1077–1091, March 2017.
- [18] J. Lee and S. Leyffer, *Mixed Integer Nonlinear Programming*. Springer Publishing Company, Incorporated, 2011.
- [19] D. W. K. Ng, Y. Wu, and R. Schober, "Power efficient resource allocation for full-duplex radio distributed antenna networks," *IEEE Trans. Wireless Commun.*, vol. 15, no. 4, pp. 2896–2911, April 2016.
- [20] E. Che, H. D. Tuan, and H. H. Nguyen, "Joint optimization of cooperative beamforming and relay assignment in multi-user wireless relay networks," *IEEE Trans. Wirel. Commun.*, vol. 13, no. 10, pp. 5481–5495, Oct 2014.
- [21] M. Grant and S. Boyd, "CVX: Matlab software for disciplined convex programming, version 2.1," <http://cvxr.com/cvx>, Mar. 2014.
- [22] C. She, C. Yang, and T. Q. S. Quek, "Cross-layer optimization for ultra-reliable and low-latency radio access networks," *IEEE Trans. Commun.*, vol. 17, no. 1, pp. 127–141, Jan 2018.
- [23] S. Boyd and L. Vandenberghe, *Convex Optimization*. New York, NY, USA: Cambridge University Press, 2004.